STEM CELLS TRANSLATIONAL MEDICINE®

TISSUE ENGINEERING AND REGENERATIVE MEDICINE

Anti-Inflammatory and Anti-Fibrotic Effects of Human Amniotic Membrane Mesenchymal Stem Cells and Their Potential in Corneal Repair

ALEJANDRO NAVAS,[a,b,*] FÁTIMA SOFÍA MAGAÑA-GUERRERO,[a,d,*] ALFREDO DOMÍNGUEZ-LÓPEZ,[a,d] CÉSAR CHÁVEZ-GARCÍA,[a] GRACIELA PARTIDO,[a] ENRIQUE O. GRAUE-HERNÁNDEZ,[b] FRANCISCO JAVIER SÁNCHEZ-GARCÍA,[c] YONATHAN GARFIAS [a,d]

[a]Research Unit, Cell and Tissue Biology, Institute of Ophthalmology Conde de Valenciana, Mexico City, Mexico; [b]Department of Cornea and Refractive Surgery, Institute of Ophthalmology Conde de Valenciana, Mexico City, Mexico; [c]Laboratorio de Inmunorregulación, Departamento de Inmunología, Escuela Nacional de Ciencias Biológicas, Instituto Politécnico Nacional, Col Santo Tomás, Mexico; [d]Faculty of Medicine, Department of Biochemistry, Universidad Nacional Autónoma de México, Mexico City, Mexico

*Contributed equally.

Yonathan Garfias, M.D., Ph.D., Department of Biochemistry, Faculty of Medicine, Universidad Nacional Autónoma de México. Av. Universidad 3000, C.P. 04510, Mexico City, Mexico. Instituto de Oftalmologia Mexico.52 (55) 5623 2168; e-mail: yogarfias@institutodeoftalmologia.org; ygarfias@bq.unam.mx

Received February 28, 2018; accepted for publication July 28, 2018; first published September 10, 2018.

http://dx.doi.org/10.1002/sctm.18-0042

Key Words. hAM-MSC • Corneal repair • α-SMA myofibroblasts • NETs • Inflammation

ABSTRACT

Acute ocular chemical burns are ophthalmic emergencies requiring immediate diagnosis and treatment as they may lead to permanent impairment of vision. The clinical manifestations of such burns are produced by exacerbated innate immune response via the infiltration of inflammatory cells and activation of stromal fibroblasts. New therapies are emerging that are dedicated to repair mechanisms that improve the ocular surface after damage; for example, transplantation of stem cells (SC) has been successfully reported for this purpose. The pursuit of easily accessible, noninvasive procedures to obtain SC has led researchers to focus on human tissues such as amniotic membrane. Human amniotic mesenchymal SC (hAM-MSC) inhibits proinflammatory and fibrotic processes in different diseases. hAM-MSC expresses low levels of classical MHC-I and they do not express MHC-II, making them suitable for regenerative medicine. The aim of this study was to evaluate the effect of intracameral injection of hAM-MSC on the clinical manifestations, the infiltration of inflammatory cells, and the activation of stromal fibroblasts in a corneal alkali-burn model. We also determined the in vitro effect of hAM-MSC conditioned medium (CM) on α-SMA$^+$ human limbal myofibroblast (HLM) frequency and on release of neutrophil extracellular traps (NETs). Our results show that intracameral hAM-MSC injection reduces neovascularization, opacity, stromal inflammatory cell infiltrate, and stromal α-SMA$^+$ cells in our model. Moreover, in in vitro assays, CM from hAM-MSC decreased the quantity of α-SMA$^+$ HLM and the release of NETs. These results suggest that intracameral hAM-MSC injection induces an anti-inflammatory and anti-fibrotic environment that promotes corneal wound healing. STEM CELLS TRANSLATIONAL MEDICINE *2018;7:906–917*

SIGNIFICANCE STATEMENT

Stem cells obtained from human amniotic membrane are capable of reducing inflammation and fibrosis in corneal chemical burns.

INTRODUCTION

The corneal epithelium is a protective barrier on the ocular surface that is essential for maintaining transparency in the cornea, allowing visual perception [1]. Acute ocular chemical burns, which are responsible for 11.5%–22.1% of ocular injuries [2], are ophthalmic emergencies, requiring immediate diagnosis and prompt treatment. Alkali burns are more severe than acid burns, as alkali reagents rapidly penetrate ocular tissues due to their lipophilic properties. During the healing process of corneal alkali burns, the injured tissue secretes proteolytic enzymes [3]. In the corneal stroma, resident keratocytes are responsible for secreting extracellular matrix components required to maintain normal corneal structure and function [4]; however, after corneal injury, quiescent keratocytes differentiate into active fibroblast and myofibroblast phenotypes. This cell transformation is critical in normal wound healing but can also be associated with aberrant corneal scar formation [5]. Moreover, it has been suggested that myofibroblasts may secrete inflammatory cytokines, growth factors, and chemokines that promote immune cell infiltrate into the cornea, which are other major contributors to corneal opacity and vision loss [5, 6]. Despite the fact that stem cell therapy is still controversial in the ophthalmological field, some studies suggest the potential benefit of mesenchymal stem cells in repairing damaged ocular structures [7, 8]. Nevertheless, solid evidence about keratocyte replacement and corneal mesenchymal

stem cells is insufficient, and more studies are needed to fully understand ocular repair mechanisms following stem cell transplantation [9–11].

Mesenchymal stem cells (MSC) are able to regenerate tissues; also, it has been widely reported that they have immunomodulatory and anti-fibrotic properties based on secretion of a myriad of paracrine molecules [12, 13]. In addition, administration of MSC significantly inhibits inflammation in various fibrotic diseases, such as lung injury, myocardial infarction, renal fibrosis, and liver cirrhosis [14–18]. MSC can be obtained from different tissues, including bone marrow, adipose tissue, dental pulp, skin, and peripheral blood. Although, bone marrow stem cells have been used extensively in several studies, their collection is associated with invasive procedures resulting in relatively low amounts of MSC, and the number of such cells falls as the donor's age increases [19].

The search for easily accessible and noninvasive procedures to obtain MSC has recently focused on other human tissues, such as amniotic membrane. Human amniotic mesenchymal stem cells (hAM-MSC) are derived from embryonic mesoderm. Cumulative evidence shows that hAM-MSC have many advantages for use as a source of allogenic cells for regenerative medicine, as they present immunosuppressive effects due to their ability to secrete immunosuppressive HLA-G [20], their low expression of MHC class I, and no expression of MHC class II antigens or costimulatory molecules in the presence of interferon-γ [21, 22]. These antecedents indicate that hAM-MSC are able to survive in immunocompatibility mismatched allogeneic transplant recipients. A previous study suggests that subconjunctival injection of hAM-MSC ameliorated corneal opacity and neovascularization in an alkali burn model; the use of hAM-MSC significantly decreased TNF-α in aqueous humor in comparison with a nontreated group, suggesting that hAM-MSC can inhibit delivery of proinflammatory factors [23]. Therefore, adequate corneal epithelialization using MSC is related to the inhibition of acute inflammation rather than their regenerative properties [24].

In the present study, we report on the ability of hAM-MSC to ameliorate clinical manifestation of alkali burns in a corneal alkali-burn model when they are administered into the anterior chamber of the eye; in addition, we show that hAM-MSC intracameral transplantation significantly reduces corneal inflammatory response, inhibiting inflammatory cell infiltrate, decreasing corneal myofibroblast differentiation, and inhibiting neutrophil extracellular traps (NETs). Interestingly, intracamerally transplanted hAM-MSC remain in the anterior chamber of the eye as long as 12 days after transplantation, which suggests that soluble factors could be responsible of their anti-inflammatory effect. Moreover, in in vitro conditions, the soluble factors of hAM-MSC are able to down-regulate α-smooth muscle actin (α-SMA) protein on primary cultures of human limbal myofibroblasts and are also able to diminish the release of NETs by human-derived neutrophils. This further suggests that the soluble factors secreted from these cells play an important role in inhibiting inflammatory processes in the cornea.

Materials and Methods

Reagents

Trypsin, collagenase II, fetal bovine serum (FBS), dispase II, phosphate buffer solution (PBS, pH 7.2), penicillin (10,000 IU/mL), and streptomycin (10 mg/mL), were obtained from Invitrogen (Waltham, MA). Dulbecco's Modified Eagle Medium/Nutrient Mixture/F-12 (DMEM/F-12), Trypan Blue, *p*-formaldehyde, poly-*L*-lysine, Triton X-100, dimethyl sulfoxide (DMSO), propidium iodide (PI), and *L*-glutamine were purchased from Sigma-Aldrich (Saint Louis, MO). Ethylenediaminetetraacetic acid (EDTA) was obtained from Promega (Madison, WI). Purified antibodies, including anti-neutrophil elastase (NE), anti—α-SMA, and anti-human nuclear antigen (HNA), were purchased from Abcam (Cambridge, England). Alexa Fluor 488- and Alexa Fluor 594-conjugated goat anti-rabbit antibodies and a Qtracker 655 cell-labeling kit were obtained from LifeTechnologies (Eugene, OR). Flourescein isothiocyanate (FITC)-conjugated goat anti-mouse antibody was obtained from Santa Cruz Biotechnology (Dallas, TX). Purified antibody Ki-67 was purchased from Cell Marque (Rockline, CA). Bovine serum albumin (BSA) was obtained from Calbiochem (San Diego, CA). T75 cell culture flasks and 24-well plastic plates were purchased from Corning Inc. (Corning, NY). Vectashield mounting medium was purchased from (Vector Laboratories (San Diego, CA). Polymorphoprep was obtained from Axis-Shield (Oslo, Norway).

Rabbit Corneal Alkali-Burn Model

New Zealand White rabbits weighing 2–2.5 kg were used in accordance with the Association for Research in Vision and Ophthalmology (ARVO) Statement for the Use of Animals in Ophthalmic and Vision Research. The protocol was approved by our Institutional Review Board (IRB). Rabbits were randomly divided into three groups. All animals were kept in pathogen-free conditions with food and water available *ad libitum* and were housed in a 12 hour light/12 hour dark cycle. All procedures were performed under deep anesthesia and all available efforts were made to prevent any pain. Six animals per group were randomly assigned as follows [25]: group 1 was used as a control group and was administered no corneal alkali-burn lesion nor hAM-MSC treatment (control group); group 2 were NaOH-injured and treated only with 300 μL of BSS which was injected into the anterior chamber of the eye (NaOH group); the rabbits in group 3 were injured with NaOH, following which 1×10^6 hAM-MSC in 300 μL of balanced salt solution (BSS) was injected into the anterior chamber of the eye (NaOH-hAM-MSC group). All the injections were performed using a 1 mL, 27-gauge syringe (BD, Mexico City, Mexico). To induce the corneal alkali-burn injury, the rabbits were anesthetized with ketamine/xylazine. After deep anesthesia, a drop of 0.5% tetracaine (Sophia, Jalisco, Mexico) was applied directly on the experimental eye of the rabbit; then, a 6 mm-diameter Whatman filter paper soaked in 0.5 N NaOH was applied to the cornea for 15 seconds, including 4/5 of the upper peripheral cornea and 1/5 of the upper limbus, followed by profuse rinsing with 10 mL of BSS. After the corneal alkali-burn model was generated and the intracameral injections were performed (groups 2 and 3), the animals received antibiotic eye drops twice daily for 12 days, at which time the animals were euthanized following ethical procedures.

Amniotic Membrane Mesenchymal Stem Cell Isolation

All methods and experimental protocols for MSC isolation were carried out in accordance with the Institutional Review Board (IRB) of the Institute of Ophthalmology Conde de Valenciana. The protocol was approved by the same IRB. Additionally, informed consent was obtained from women who voluntarily donated their placentas. Human term placentas were processed immediately after delivery. All donors included in this study were

18 years old or older, and the criteria for donation were similar to those reported by Chávez-García et al. [26]. The cells were obtained as previously described, with slight modifications [27–29]. Briefly, the chorion was separated from the amnion and discarded, while the amnion was incubated with trypsin–EDTA at 37°C to release the amniotic epithelial cells. Amniotic membrane (AM) mesoderm digestion was performed using 0.75 mg/mL of collagenase II for 90 minutes at 37°C under vigorous agitation. The enzymatic reaction was stopped by adding growth media supplemented with 10% FBS, antibiotics, and 1% *L*-glutamine. The cell suspension was passed through a 100 μm nylon cell filter. After filtration, the suspension was centrifuged at 500× *g* for 5 minutes at 4°C and the pellet containing the cells was suspended on growth medium supplemented with 20% FBS antibiotics and 1% *L*-glutamine. The cells were cultured until they reached 90% confluence at 37°C, 5% CO_2, and 95% humidity; medium was replaced with fresh medium every 3 days. Throughout the cell culture period, the cells were microscopically observed to identify their fibroblastoid morphology. All assays were carried out with cells grown in between 3 and 6 passages.

Injection of Labeled hAM-MSC

Before intracameral injection, the hAM-MSC were obtained and labeled with quantum dot (QD) fluorescent particles following the manufacturer's instructions. Briefly, fluorescent nanoparticles (10 nM) in 0.2 mL of fresh complete growth medium were added to a microcentrifuge tube and vortexed for 30 seconds, followed by addition of 1×10^6 hAM-MSC. The sample was incubated at 37°C for 90 minutes and then washed twice with complete growth medium; labeled live cells were visualized using an ApoTome-II microscope and analyzed using Axiovison 2.0 software from Carl Zeiss (Jena, Germany). The labeled cells were suspended in fresh medium without FBS. hAM-MSC (1×10^6/300 μL) were injected into the anterior chamber immediately after corneal alkali-burn injury (NaOH-hAM-MSC group); a control group was also alkali-burn treated but the anterior chamber of the eye was injected only with 300 μL of BSS (NaOH group). All rabbits were maintained under general anesthesia during the intervention period.

Clinical Evaluation

Clinical evaluation was performed by direct observation. Clinical photographs were taken at days 1, 5, 9, and 12. The criteria for corneal opacity were as follows: grade 0, totally clear, with no opacity seen by any method of slit-lamp microscopic examination; grade 1, haze of minimal density seen with difficulty with direct and diffuse illumination; grade 2, mild haze easily visible with direct focal slit illumination; grade 3, moderately dense opacity that partially obscured the iris details; and grade 4, severely dense opacity that completely obscured the details of intraocular structures. Similarly, corneal neovascularization was scored as follows: grade 0, no intracorneal vessels, normal corneoscleral limbus; grade 1, less than five vascular loops, no longer than 0.3 mm; grade 2, from 5 to 15 vascular loops, no longer than 0.3 mm; grade 3, more than 15 vessels or loops longer than 0.3 mm; and grade 4, two or more loops longer than 0.5 mm [30, 31].

Intraocular Pressure (IOP) Determination. IOP was measured in baseline conditions (before alkali-burn model/hAM-MSC injection) and posttreatment. IOP measurements were performed using a handheld tonometer, TonoVet (Icare, Helsinki, Finland). A drop of tetracaine solution was placed on the rabbit's eye before each measurement. TonoVet measurements were performed according to Ma et al. [32] Briefly, the central groove of the tonometer was kept in a horizontal position and the distance was maintained at 4–8 mm between the tip of the probe and the cornea. Six consecutive measurements were taken, and the resulting IOP was displayed.

Assessment of Corneal Thickness Using Ultrahigh Resolution Optical Coherence Tomography (OCT). One drop of tetracaine ophthalmic solution was administrated before the OCT scan. The Visante anterior segment OCT (Carl Zeiss Meditec, Dublin, CA) was used to image the central corneas.

Histological Examination and Immunohistochemistry

After 12 days of chemical corneal burn, all animals were ethically euthanized. The corneas were carefully dissected and observed for inflammatory cell infiltration. Briefly, the tissues were fixed with 10% formalin overnight and 5 μm sections were cut and mounted onto glass slides; the samples were hematoxylin and eosin stained and observed by direct light microscope. At least three random microscopic fields at 100× magnification on each independent assay were counted by two independent observers, and acceptable interobserver and intraobserver agreement was checked and met (kappa values >0.8). Outcome histological variables included corneal edema, expressed as central corneal thickness measured in micrometer (μm) and evaluated by means of histomorphometry, and increase in stromal cells, such as fibroblasts and inflammatory cells.

Immunofluorescence Assays. For immunofluorescence assays, corneal tissues were deparaffinized and antigen retrieval was performed using 10 mM citrate buffer for 10 minutes at 60°C followed by rinsing with washing buffer (PBS pH 7.2). Tissues were then incubated with blocking buffer (PBS pH 7.2, Triton X-100, 0.1%, BSA 5%) for 2 hours at room temperature. Afterward, tissue sections were incubated overnight at 4°C with anti-α-SMA, anti-Ki-67, anti-NE, or anti-HNA primary antibodies, respectively, to identify myofibroblast differentiation, proliferating stromal cells, neutrophils, and hAM-MSC. Subsequently, the slides were rinsed 3 times with washing buffer and incubated with Alexa Fluor 488- or FITC-secondary antibodies for 2 hours at room temperature. Negative controls were performed by leaving out the primary antibodies. The cells were finally rinsed with washing buffer and mounted with DAPI-Vectashield antifade mounting medium. The corneal tissues were observed in an Apotome-II microscope (Carl Zeiss). The photographs were taken and analyzed using AxioVision Software 2.0 (Carl Zeiss).

Isolation of Human Neutrophils

Human neutrophils were isolated by density gradient from peripheral blood obtained from healthy donors, as previously described [33], with slight modifications. All the methods and experimental protocols were carried out in accordance with ERB guidelines from the Institute of Ophthalmology Conde de Valenciana. Informed consent was obtained from healthy volunteers. EDTA-anticoagulated blood was carefully added to a similar volume of polymorphoprep (v/v). After continuous centrifugation for 35 minutes at room temperature at 500× *g*, the interphase containing the granulocytes was aspirated and

transferred to a new tube and then washed twice with PBS. By this method of purification, we obtained a purity of ≥98%, as assessed by $CD11b^+/CD45^+$ staining (data not shown). Neutrophil counts and viability were evaluated using the Trypan Blue exclusion method; to avoid unspecific activation, neutrophils were kept at 4°C until they were used.

Preparation of Conditioned Medium (CM) from hAM-MSC

The CM from hAM-MSC was obtained from 1×10^6 hAM-MSC/10 mL adhered in a T75 culture flask; after FBS deprivation for 12 hours, the cells were cultured for an additional 24 hours to allow them to secrete their soluble factors.

In Vitro Stimulation and Quantification of NETs Release

Isolated neutrophils (4×10^4) were added to poly-*L*-lysine charged glass coverslips over 15 minutes at 37°C. Previously, appropriate kinetics were performed to obtain the optimal time (3 hours) and concentration (80 nM) of phorbol-12-myristate-13-acetate (PMA) to induce release of NETs (data not shown). Therefore, three groups were used in these assays: [1] neutrophils without PMA stimulation (control), [2] neutrophils with PMA stimulation (activated neutrophils), and [3] PMA-stimulated neutrophils in the presence of CM from hAM-MSC (CM hAM-MSC). To identify NETs release, isolated neutrophils in the aforementioned conditions were fixed with 4% *p*-formaldehyde for 10 minutes at room temperature and incubated with blocking buffer for 2 hours at room temperature; afterward, the cells were incubated with anti-NE overnight at 4°C. Then, the samples were rinsed and incubated with Alexa Fluor 488-conjugated goat anti-rabbit antibodies for 2 hours at room temperature, the cells were rinsed, and finally, the DNA was visualized with PI. The samples were analyzed by using an Apotome-II microscope. For each condition, five randomly selected images were acquired and used for quantification of NETs releasing cells. The image files were loaded as separate image stacks for each channel in ImageJ software. To quantify the traps, the brightness and contrast were first adjusted to every image to visualize each NET (composed of extracellular NE and DNA). Binary images were then generated and the threshold was subtracted. Subsequently, automatic particle analysis was set to a minimum size of 20 pixels. The summarized result was considered as the area occupied by the NETs released. Data were expressed as fold change of NETs-releasing cells in relation to the cells without PMA, as previously reported with modifications [29, 34]. The data are expressed as the mean of occupied area ± standard error (*SE*).

Analysis of the Effect of Secreted Factors from hAM-MSC on the Frequency of α-SMA^+ Human Limbal Myofibroblasts

Human limbal myofibroblasts (HLM) were isolated as previously described [35]. Cell purity was verified by flow cytometry using vimentin (≥90% cells were positive to vimentin, data not shown). The HLM (1×10^5 cells per well) were cultured on a 24-well cell culture plate until they were attached; afterward, the medium was changed to medium without FBS. Then, HLM were cultured in the presence of fresh growth medium without FBS or CM from hAM-MSC during 12 hours. The HLM were collected to determine the effect of CM on the expression of α-SMA by means of flow cytometry.

Flow Cytometry Assays to Identify α-SMA in HLM. Flow cytometry assays were carried out to identify the HLA α-SMA^+ frequency. Briefly, HLM under the aforementioned conditions were harvested via trypsinization and fixed with 4% *p*-formaldehyde for 10 minutes at 4°C; then, HLM were washed with PBS and incubated with permeabilization buffer (1% saponin, 10% BSA, and 0.1% NaN_3) for 20 minutes at room temperature with constant agitation. The HLM were incubated with anti-α-SMA antibody for 30 minutes at 4°C and then washed with PBS and incubated with Alexa Fluor 488-conjugated goat anti-rabbit IgG for 30 minutes at 4°C in the dark; HLM without primary antibody but with the Alexa Fluor 488-conjugated goat anti-rabbit IgG were used as the negative control for staining; cells (1×10^4) were acquired by a FACSVerse flow cytometer (BD) and analyzed using Flowjo 7.0 software.

Statistical Analysis

The data were expressed as mean ± *SE*. Student *t* tests and analysis of variation (ANOVA) tests were performed; values of $p < .05$ were considered statistically significant. Statistical analysis was carried out using GraphPad Prism 5 software (La Jolla, CA).

Results

Characterization of Human Amniotic Membrane Stromal Cells

After cell expansion in plastic culture flasks, and according to the criteria proposed by the First International Workshop on Placenta Derived Stem Cells [22], the cells obtained from the amniotic mesoderm attached to the plastic, adopting a fibroblastoid shape; these cells had the capacity to develop embryonic bodies. To determine the ability of these cells to differentiate into other tissue lineages, they were cultured in the presence of two differentiation media for 3 weeks and immunocytochemistry assays were performed. When the hAM-MSC were cultured in the presence of hepatogenic medium, they were able to express albumin; similarly, when the cells were cultured in the presence of chondrogenic medium, the cells were positive for collagen-II. Furthermore, the hAM-MSC were positive (>90%) for the following cell-surface antigens associated with mesenchymal lineage: CD29, CD44, CD73, CD90, and CD105. In contrast, hAM-MSC were negative (<3%) for expression of CD45 and CD34 hematopoietic cell markers. In addition to these results, the cells expressed the intracellular embryonic/pluripotent stem cell markers Oct-4 and SSEA-4 (Supporting Information Figures S1 and S2).

Corneal Alkali-Burn Clinical Signs Were Ameliorated Following Intracameral hAM-MSC Transplantation

We sought to determine the effect of hAM-MSC in terms of ameliorating the clinical signs (corneal opacity and neovascularization) of corneal burns in rabbits. In one group of rabbits, hAM-MSC were intracamerally injected immediately after corneal injury (NaOH-hAM-MSC group); in another group of rabbits, 300 μL of fresh growth medium without FBS was intracamerally injected immediately after corneal injury (NaOH group); the final group of rabbits received no injury and likewise did not receive any intracameral injection (control group).

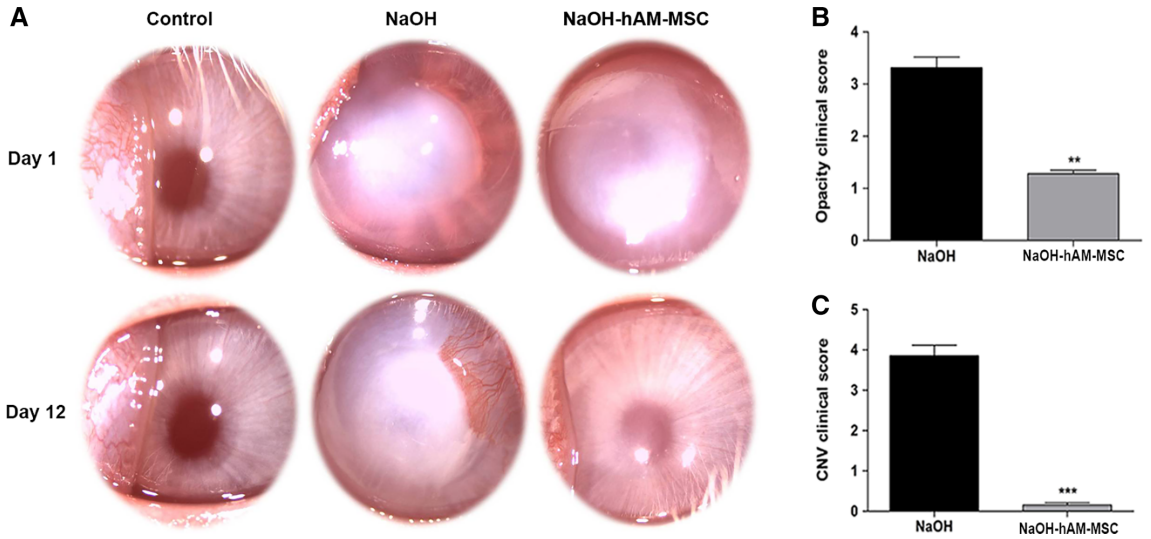

Figure 1. Intracameral **hAM-MSC** injection ameliorates neovascularization and corneal opacity on corneal burn. Clinical photographs of non-injured cornea of control group (top and bottom-left plots); alkali-injured cornea of **NaOH** group and treated with intracameral **BSS** (top and bottom-middle plots); and alkali-injured cornea of **NaOH-hAM-MSC** group (top and bottom-right plots) at day 1 (top plots) and 12 days after burn (bottom plots). Notice that **hAM-MSC** injection ameliorates clinical features of the alkali-corneal burn injury 12 days after the intracameral injection of **hAM-MSC**. These are representative images of six independent assays (A). Graphical comparison of corneal opacity (B) and corneal neovascularization (C) scores, among **NaOH** and **NaOH-hAM-MSC** treated groups. Intracameral injection of **hAM-MSC** (grey bars) reduces significantly corneal opacity (**p < .01; n = 6); and corneal neovascularization (***p < .001; n = 6) in comparison with alkali-burned corneas (black bars). These results are obtained from the clinical evaluation at day 12 postinjury. Data are expressed as the mean value of clinical score ± SE. Abbreviation: CNV, corneal neovascularization.

As expected, 12 days after corneal injury, the NaOH group presented the highest corneal neovascularization score (4.11 ± 0.26); interestingly, the injection of hAM-MSC (NaOH-hAM-MSC group) significantly inhibited corneal neovascularization (0.15 ± 0.05) measured for the same period of time in comparison with the NaOH group (p < .05). When corneal opacity was measured 12 days after injury, similar results were obtained: the NaOH group presented the highest corneal opacity score (3.21 ± 0.34), while the group injected with hAM-MSC (NaOH-hAM-MSC group) showed a significant (p < .05) decrease in corneal opacity score (1.24 ± 0.06) in comparison with the NaOH group. In the control group of rabbits, there were no changes in the corneal neovascularization or in the corneal opacity (Figure 1).

Intracameral hAM-MSC Injection Diminished IOP

To determine the effect of the intracameral injection of hAM-MSC on IOP, measurements were collected with a TonoVet veterinary tonometer. All rabbits presented a baseline mean IOP value of 11.2 ± 0.6 mmHg; 12 days after treatment, the mean IOP values of the NaOH group increased to 14.66 ± 0.8 mmHg, which was significantly different from the baseline mean IOP values (p < .05). In contrast, the mean IOP values of the NaOH-hAM-MSC group 12 days posttreatment was 10 ± 0.5 mmHg; although there was no difference when compared with the mean baseline IOP values (p > .05), it was significantly different (p < .05) when compared with the mean IOP values of the NaOH group at the same time point (Table 1).

Intracameral hAM-MSC Injection Reduced in vivo Corneal Edema

To evaluate the effect of intracameral injection of hAM-MSC in in vivo corneal edema, the corneal thickness of all animals was measured by means of anterior OCT. The extent of edema caused by the corneal alkali-burn was determined immediately after the NaOH treatment, and the OCT measurements showed a central corneal thickness of 489 ± 18 μm in both NaOH and NaOH-hAM-MSC groups. Interestingly, 12 days postinjury and treatment, the NaOH hAM-MSC group presented a significant reduction (p < .05) in central corneal thickness (373 ± 13.6 μm) with respect to the central corneal thickness of the NaOH group (412 ± 9.2 μm) at the same time point. The control group presented a corneal thickness of 370 ± 6.3 μm, which, while statistically different from the NaOH group (p < .05), was not statistically different from the NaOH hAM-MSC group (p > .05) (Table 1 and Supporting Information Figure S3).

Intracameral hAM-MSC Injection Diminished Histological Features of Corneal Inflammation

Histological analyses performed on hematoxylin and eosin stained samples of the corneas subjected to the aforementioned conditions showed that while the number of cells with dark stained nuclei (representing inflammatory leukocytes)

Table 1. hAM-MSC decreased in vivo edema and intraocular pressure on alkali-burn model

	Control group	NaOH group (n = 6 eyes)	NaOH-hAM-MSC group (n = 6 eyes)	*p value
Inflammatory cells per field	0.2 (±0.5)	12.6 (±0.8)	3.8 (±1.3)	.0040
Corneal thickness (μm)	323 (±30.6)	489 (±31.5)	408 (±8.2)	.0325

*p value represents statistical difference between NaOH versus NaOH-hAM-MSC treated groups. One-way ANOVA tests were performed.

Table 2. hAM-MSC reduce clinical injury on alkali-burn model

	Control group	NaOH group (n = 6 eyes)	NaOH-hAM-MSC group (n = 6 eyes)	*p value
OCT (μm)	370 (±6.3)	412 (±9.2)	373 (±13.6)	.04
IOP (mmHg)	11.2 (±0.6)	14.7 (±0.8)	10 (±0.5)	.01

*p value represents statistical difference between NaOH versus NaOH-hAM-MSC treated groups. One-way ANOVA tests were performed. Abbreviations: OCT, optical coherence tomography; IOP, intraocular pressure.

was negligible in the control group, there was a significant increase in their number in the NaOH group; in contrast, the number of these dark stained nuclei cells representing leucocyte infiltration decreased significantly ($p < .05$) in the corneas of the NaOH-hAM-MSC group. Similarly, corneal edema increased ($p < .05$) when the tissue was NaOH injured and treated only with BSS in comparison with the control group; interestingly, intracameral injection of hAM-MSC was followed by a significant reduction ($p < .05$) in corneal edema in comparison with the NaOH group ($p < .05$); however, it did not differ ($p > .05$) from the control group (Table 2).

Tracking hAM-MSC in the Anterior Chamber After Corneal Chemical Injury

To determine the capacity of hAM-MSC to transdifferentiate to corneal epithelium, we tracked QD-labeled hAM-MSC by means of immunofluorescence at day 12 after intracameral injection. Interestingly, no QD-labeled hAM-MSC was observed in the corneal tissue; QD-hAM-MSC were located only in the iris, suggesting that hAM-MSC secrete soluble factors that inhibit both the corneal inflammatory process and the differentiation of myofibroblasts within the stromal cornea. To confirm that QD fluorescent (655 nm) particles were still present in the injected hAM-MSC, we performed staining with a specific human nuclear antigen (HNA), and we found double positive cells in the iris (Figure 2, Supporting Information Figure S4).

Intracameral hAM-MSC Injection Reduced Corneal Stromal Myofibroblast Differentiation and Proliferation of Corneal Stromal Cells

Immunofluorescence assays were performed to determine proliferation of stromal cells (Ki-67$^+$ cells) and differentiation of myofibroblasts (α-SMA$^+$ cells). As expected, the number of Ki-67$^+$ cells in the stromal cornea of the control group was negligible, whereas the NaOH group showed a significant ($p < .05$) increase in Ki-67$^+$ cells in the stroma of the cornea in comparison with the control group. The number of Ki-67$^+$ cells in the corneal stroma from the NaOH-hAM-MSC group was significantly reduced ($p < .05$) in comparison with the NaOH group (Figure 3). Like-wise, the number of α-SMA$^+$ cells in the corneal stroma of the control group was negligible; in contrast, the number of α-SMA$^+$ cells in the corneal stroma significantly increased ($p < .05$) in the NaOH group in comparison with the control group. Interestingly, the α-SMA$^+$ cells in the corneal stroma significantly decreased ($p < .05$) in the NaOH-hAMSC group in comparison with the NaOH group, suggesting that intracameral injection of hAM-MSC is able to inhibit myofibroblast differentiation of keratocytes in a corneal chemical burn model (Figure 4).

Soluble Factors of hAM-MSC Significantly Reduced the Frequency of α-SMA$^+$ HLM

To determine the effect of the soluble factors secreted by the hAM-MSC on α-SMA$^+$ HLM (we considered HLM as limbal fibroblasts with low levels of α-SMA), HLM were isolated from a cadaveric donor and cultured in the presence of hAM-MSC conditioned medium (CM). After HLM were seeded in the presence or absence of hAM-MSC CM, the α-SMA$^+$ HLM were evaluated via flow cytometry. After 12 hours in the presence of non conditioned culture medium without FBS, the percentage of α-SMA$^+$

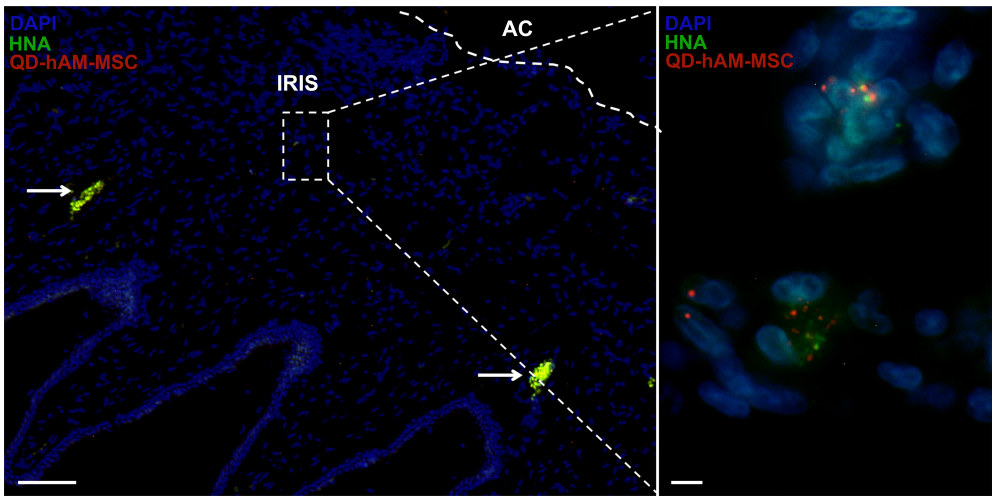

Figure 2. **hAM-MSC** locate into the anterior chamber after 12 days of intracameral injection. Fluorescence microscopy of the anterior chamber of an **NaOH-hAM-MSC** treated cornea. The **hAM-MSC** was **QD-labeled** and injected intracamerally at the same time of corneal injury. After 12 days, immunofluorescence microscopy was performed to visualize **HNA** marker. Interestingly, **hAM-MSC** were found in the iris even after 12 days of injection and were not located in the cornea or adjacent tissues such as corneal endothelium or ciliary processes; arrows indicate the autofluorescence of erythrocytes (left plot, scale bar represents 100 μm); the magnification of inner square is presented in right plot (scale bar represents 5 μm). In both plots cell nuclei are shown with **DAPI** (blue), **QD-labeled-hAM-MSC** in red and **HNA** marker in green. These are representative images from six-independent assays. Abbreviations: AC, anterior chamber; DAPI, 4′,6-diamidino-2-phenylindole; hAM-MSC, human amniotic mesenchymal stem cell; HNA, human nuclear antigen; QD, quantum dot.

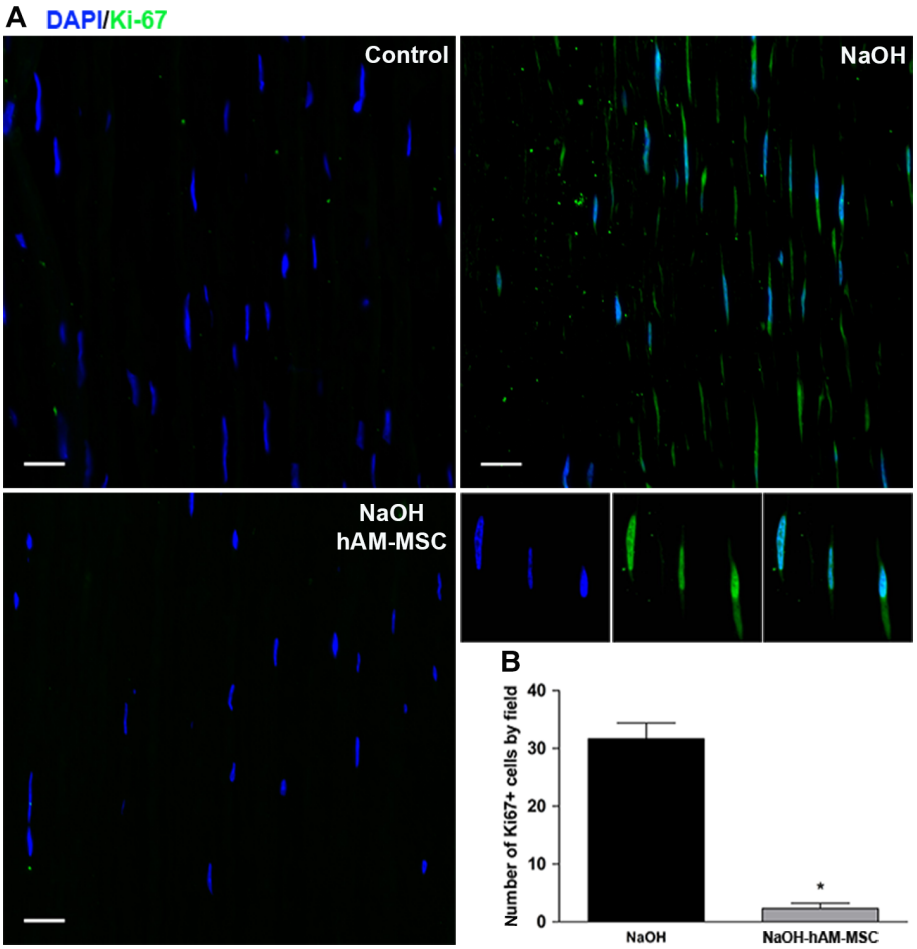

Figure 3. Intracameral **hAM-MSC** injection diminishes stromal cell proliferation. Immunofluorescence micrographs from the corneal stroma stained with the proliferating cell marker **Ki-67** in the control group (top-left plot), **NaOH-group** (top-right plot) and **NaOH-hAM-MSC** group (bottom-left plot). **Ki-67** is preferentially expressed into the nucleus of the stromal proliferating cells as shown in the middle right plots. These are representative images from six-independent experiments; scale bar represents 20 μm (A). The chemical burn induces a significant augmentation of the **Ki-67$^+$** cells in the corneal stroma in comparison with the control group; interestingly, the **NaOH-hAM-MSC** group presented a significant reduction in comparison with the **NaOH-group** as observed in the bars graphic (bottom-right plot) (B). Three random fields were analyzed for each animal (n = 6). Data are expressed as mean ± SE (*p < .05).

HLM was 68% ± 9%, whereas the presence of CM from hAM-MSC for 12 hours significantly reduced the percentage of α-SMA$^+$HLM to 40% ± 12% (p < .05) (Figure 5, Supporting Information Figure S5), suggesting that soluble factors secreted from hAM-MSC could reverse differentiated HLM back to fibroblasts.

Soluble Factors Secreted from hAM-MSC Reduced the Release of NETs by Human-Derived Neutrophils

Inflammatory infiltrate cells in corneal stroma from the NaOH-injured group were identified as neutrophils as determined by anti-NE antibody; these cells were able to release structures resembling NETs (Supporting Information Figure S6); therefore, we decided to determine whether soluble factors secreted from hAM-MSC affected release of NETs. Consequently, we isolated neutrophils from human peripheral blood and stimulated them or not with PMA in the presence or not of hAM-MSC CM. When the neutrophils were PMA-activated in the presence of fresh culture medium without FBS, there was a fourfold increase in NETs-releasing cells in comparison with non-stimulated neutrophils (p < .05). Although, there was an increase in NETs-releasing cells when PMA-stimulated neutrophils were cultured, in the presence of CM, in comparison with the nonstimulated neutrophils (p < .05), there was a significant reduction (p < .05) of NETs-releasing cells in comparison with the PMA-stimulated isolated neutrophils cultured in the absence of CM. These results suggest that hAM-MSC secretes soluble factors that inhibit the release of NETs by activated neutrophils (Figure 6).

Discussion

In the present study, we showed that hAM-MSC injected into the anterior chamber of the eye ameliorated the clinical and histopathological manifestations of injury in a corneal alkali-burn model. Moreover, in in vitro assays, hAM-MSC CM is able to diminish human keratocyte differentiation and reduce the release of NETs by human-derived neutrophils. These findings suggest that hAM-MSC possess anti-inflammatory and anti-fibrotic properties. Several studies have shown corneal regeneration using MSC obtained from bone marrow, adipose tissue, umbilical cord, umbilical cord blood, and dental pulp, among many other tissues [36–40]. In this context, MSC obtained from human amniotic membrane have previously been used as a potential therapeutic tool in cardiovascular,

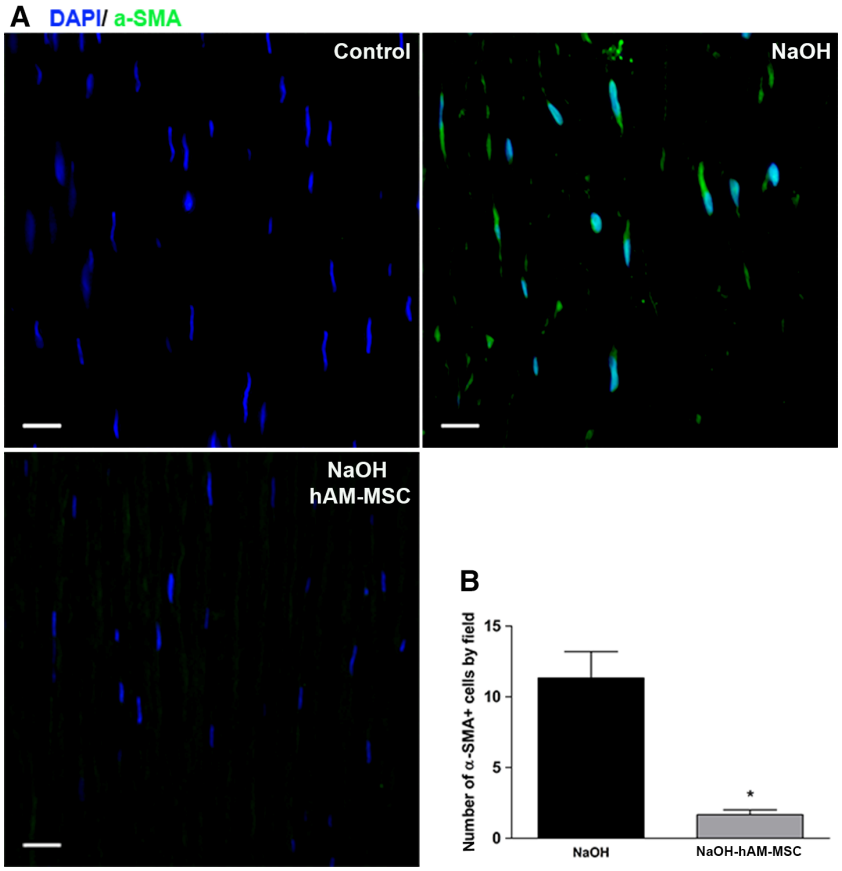

Figure 4. Intracameral **hAM-MSC** injection reduces corneal myofibroblasts differentiation. Immunofluorescence micrographs from the corneal stroma stained with **anti-α-SMA** in the control group (upper-left panel), **NaOH group** (upper-right panel) and **NaOH-hAM-MSC** (lower-left panel). These are representative images from six independent experiments, scale bar represents 20 μm (A). Interestingly, the group of the alkali-injured rabbits treated with **hAM-MSC** (grey bar) presented a significant reduction of the **α-SMA** positive cells in comparison with the alkali-burned group (black bar) as observed in the bars graphic (lower-right panel) (B). Three random fields were analysed for each animal (n = 6). Data are expressed as mean ± SE (*$p < .05$).

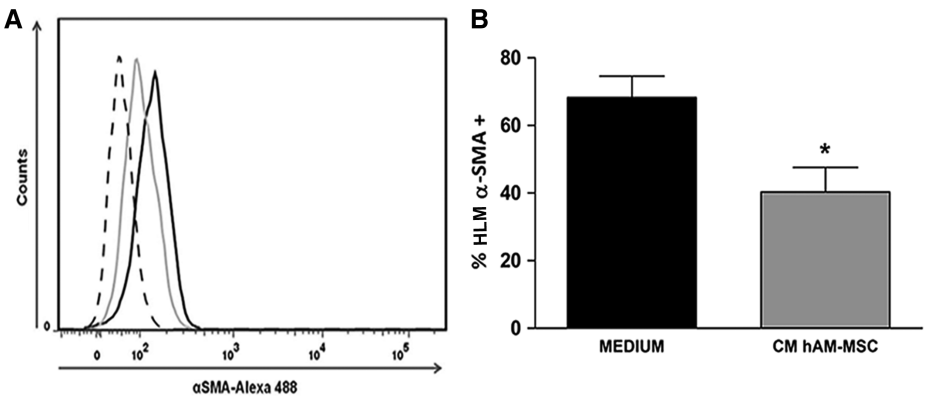

Figure 5. **CM** from **hAM-MSC** significantly reduces the frequency of **α-SMA$^+$ HLM**. Histograms from human limbal myofibroblasts **(HLM)** cultured in the presence (gray line) or in the absence (black line) of **CM** from **hAMSC** during 12 hours; dashed line represents the staining negative control (A). **CM** from **hAM-MSC** significantly reduce the frequency of **α-SMA$^+$ HLM** (gray bar) compared with the **α-SMA$^+$ HLM** incubated only with medium (black bar) (B). Each bar represents the mean of **α-SMA$^+$ HLM** frequency ± SE (*$p < .05$; n = 3).

hepatic, and osteoarticular diseases [20, 41, 42]. The cells obtained from the mesoderm of amniotic membrane in this study are stromal stem cells, as demonstrated by their fibroblastoid morphology, adherence to plastic, formation of embryonic bodies, expression of markers, and capacity to transdifferentiate into other cell linages; these features are in accordance with those proposed by the First International Workshop on Placenta Derived Stem Cells (shown in Supporting Information Figures S1 and S2) [22]. It has been proposed that MSC tend to home in on damaged tissues and are able to migrate specifically to inflamed tissues [43]. In this context, there is evidence demonstrating the effectiveness of transplanting bone marrow MSC (BM-MSC), by different routes, in corneal alkali-burn models. It has been shown that systemic injection of BM-MSC into the ear 24 hours before injuring the cornea is able to

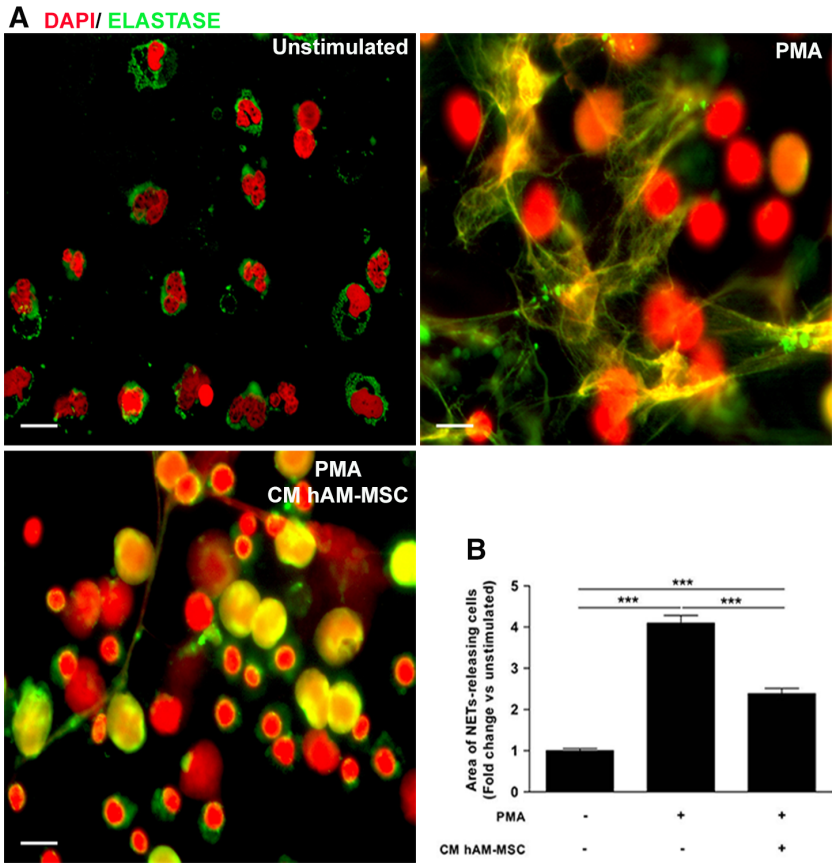

Figure 6. **CM** from **hAM-MSC** reduced **NETs** releasing cells. Human isolated neutrophils were stimulated or not with **PMA** and **NETs** release was identified with extracellular **DNA** and elastase. Nonstimulated neutrophils present their characteristic lobulated nuclei and the elastase were located in the cytoplasm (top-left plot); in contrast, **PMA-stimulated** neutrophils liberated **NETs** identified by the colocalization of both **DNA** and elastase (top-right plot); meanwhile, **PMA-stimulated** neutrophils cultured in the presence of **CM** from **hAM-MSC**, presented nonlobulated nuclei and the release of **NETs** by these cells was reduced (bottom-left plot). The images are representative of three independent assays; scale bar represents 20 μm (A). **PMA** increased **NETs** release up to fourfold change in comparison with the nonstimulated neutrophils; in contrast, and interestingly, CM from **hAM-MSC** was able to significantly reduce **NETs** release in **PMA-stimulated** neutrophils (bottom-right plot) (B). Data are expressed as mean ± SE (***$p < .001$).

promote healing in a corneal alkali-burn model [44]; similar results were obtained when BM-MSC were seeded on artificial scaffolds and transplanted on the conjunctiva in an alkali corneal-burn model [45]; these results demonstrate that different methods of application of BM-MSC are effective.

As far as we know, very few studies have shown the potential of hAM-MSC to regenerate corneal tissue, and to our knowledge this is the first study using hAM-MSC intracameral injection as a therapy for corneal inflammation. In our study, we show that intracameral application of hAM-MSC represents a novel route of administration that is capable of generating corneal recovery and reducing stromal inflammation in a chemical corneal burn model. In addition, hAM-MSC injection was able to significantly reduce in vivo edema in the alkali-burned corneas, as measured via OCT and corroborated by histomorphometry; in this context, previous study demonstrated that these two techniques provide equivalent results [46].

There are still controversies regarding whether MSC cells are able to differentiate into healthy cell tissue or whether their secreted soluble factors have an effect on the recovery of damaged tissues. To solve this issue, we administered QD-labeled hAM-MSC into the anterior chamber of the eye. Interestingly, even in follow-up 12 days posttreatment, the QD-labeled hAM-MSC were found in the iris and colocalized with a human antigen, supporting their human origin; these results are in accordance with those reported by Roubeix et al., who described that BM-MSC were still present in the corneal endothelium, iris, ciliary processes, and trabecular meshwork 3 weeks postintracameral injection [47], suggesting that the secreted soluble factors are in part responsible for this effect.

To determine whether the intracameral hAM-MSC injection had an effect on intraocular pressure, IOP measurements were taken with a TonoVet; interestingly, in contrast to the chemically injured eyes treated only with BSS, which presented high IOP values [48], the chemically injured eyes that received hAM-MSC presented significantly lower IOP pressures, similar to that of the control eyes, suggesting that this novel route of administration is safe. Furthermore, these results strengthen the proposal that MSC transplantation is an effective tool for treating ocular hypertension [47, 49].

The α-SMA expressing myofibroblasts are the main cells participating in corneal wound healing. During corneal wound healing, fibroblastic precursors on corneal stroma begin their differentiation to myofibroblasts; at the same time, the secretion of transforming growth factor-β (TGF-β) regulates the intracellular expression of α-SMA, which allows myofibroblasts to participate in the

extracellular matrix organization [50, 51]. However, the deposition of disorganized extracellular matrix compounds secreted by myofibroblasts, along with the disorder of the collagen fiber of the corneal stroma and the release of inflammatory cytokines, growth factors, and chemokines, are the major contributors to the induction of corneal opacity [6]. Moreover, it has been reported that α-SMA$^+$ myofibroblasts are the cells mainly responsible for promoting corneal haze and opacity in murine models [52]. The decrease in the number of Ki-67$^+$ and α-SMA$^+$ cells in the corneal stroma upon injection of hAM-MSC suggests that soluble factors secreted by hAM-MSC have an anti-fibrotic effect by decreasing the proliferation of myofibroblasts. Whether soluble factors from hAM-MSC inhibit the TGF-β pathway is still a matter of study [53].

To confirm that soluble factors from hAM-MSC were responsible for the anti-inflammatory and anti-fibrotic effects seen in the rabbit cornea, we collected the CM from hAM-MSC and performed in vitro assays with HLM. The HLM constitutively expressed the α-SMA protein; however, culturing HLM with CM of hAM-MSC decreased the percentage of α-SMA$^+$ HLM; the aforementioned results confirm the suppressive effect of the soluble factors of hAM-MSC in the transdifferentiation of fibroblasts to myofibroblasts. We have previously shown that deepithelialized amnion is able to interact with HLM, inhibiting NF-κB nuclear translocation [35]; likewise, the amniotic membrane extract is able to inhibit myofibroblasts differentiation [53].

Contributors to corneal opacity other than fibrotic conditions include inflammatory mediators. Neutrophils are inflammatory immune cells that are able to migrate through tissues, infiltrate them, and participate in inflammatory processes. One of the effector mechanisms of neutrophils that has been associated with the development of damage and inflammation in tissues is the release of NETs. NETs are structures formed by nuclear components such as extracellular DNA and histones, as well as cytoplasmic proteases, antimicrobial peptides, and oxidant molecules [54, 55]. The exacerbated release of NETs contributes to the development and maintenance of inflammatory ocular processes, such as dry eye disease, and diabetic retinopathy, and is the cause of antineutrophil cytoplasmic antibody (ANCAS)-associated vasculitis [56–58]. Other reports have indicated that the secretion of inflammatory cytokines, metalloproteases, gelatinase, and mieloperoxidase, as well as increased neutrophil infiltrate, are major participants in deterioration of wound healing in corneal alkali-burn models [59, 60]. It is shown here that the corneal tissue of rabbits with alkali-burn injury showed an increase in the number of inflammatory cells, mainly neutrophils; also, we identified that these infiltrating cells released NETs (Supporting Information Figure S4); interestingly, those rabbits that received the hAM-MSC injection showed a significant reduction in the number of infiltrating cells. These results suggest that neutrophils play an important role in corneal inflammation and that hAM-MSC have an immunosuppressive effect over neutrophils and their effector mechanisms. In this context, the CM obtained from hAM-MSC was able to reduce the release of NETs by human-derived neutrophils in vitro. It has been shown that MSC synthesize and secrete many factors that modulate the inflammatory response. Some of the immunosuppressive molecules secreted by the hAM-MSC are IL-10, TGF-β, and IDO, and recently we have demonstrated that TSG-6 secreted by hAM-MSC is able to reduce the release of NETs by bone marrow-derived murine neutrophils [29]. Therefore, it is likely that TSG-6 is also involved in the observed healing in the corneal alkali-burn model [61].

Conclusion

In conclusion, intracameral hAM-MSC injection could be a plausible alternative treatment for corneal repair in cases of severe ocular surface diseases.

Acknowledgments

This work is part of the Doctoral Thesis of A.N. who received a scholarship from CONACYT-CVU: 277499. F.S.M.G. received a scholarship from CONACYT-CVU: 406452. This work was supported by a grant from CONACYT-CIENCIA BASICA-167438, CONACYT-Problemas Nacionales 311, UNAM-PAPIIT-DGAPA: IN215617; and Conde de Valenciana Foundation.

Author contributions

A.N.: conception and design, collection and assembly of data, data analysis and interpretation, manuscript writing, and final approval of manuscript; F.S.M.-G.: Conception and design, collection and assembly of data, data analysis and interpretation, manuscript writing, and final approval of manuscript; A.D.-L.: Collection and assembly of data, data analysis and interpretation, and final approval of manuscript; C.C.-G.: Collection and assembly of data, data analysis and interpretation, and final approval of manuscript; G.P.: Collection and assembly of data, data analysis and interpretation, and final approval of manuscript; E.O.G.-H.: Provision of study material and patients, collection and assembly of data, data analysis and interpretation, and final approval of manuscript; F.J.S.-G.: Data analysis and interpretation, manuscript writing, and final approval of manuscript; Y.G.: Conception and design, provision of study materials, data analysis and interpretation, manuscript writing, and final approval of manuscript.

Disclosure of Potential Conflicts of Interest

The authors indicated no potential conflicts of interest.

References

1 Meek KM, Knupp C. Corneal structure and transparency. Prog Retin Eye Res 2015; 49:1–16.

2 Clare G, Suleman H, Bunce C et al. Amniotic membrane transplantation for acute ocular burns. Cochrane Database Syst Rev 2012;12:CD009379.

3 Baradaran-Rafii A, Eslani M, Haq Z et al. Current and upcoming therapies for ocular surface chemical injuries. Ocul Surf 2017;15:48–64.

4 Petroll WM, Lakshman N, Ma L. Experimental models for investigating intra-stromal migration of corneal keratocytes, fibroblasts and myofibroblasts. J Funct Biomater 2012;3: 183–198.

5 Myrna KE, Mendonsa R, Russell P et al. Substratum topography modulates corneal fibroblast to myofibroblast transformation. Invest Ophthalmol Vis Sci 2012;53:811–816.

6 Torricelli AA, Wilson SE. Cellular and extracellular matrix modulation of corneal stromal opacity. Exp Eye Res 2014;129: 151–160.

7 Dhamodaran K, Subramani M, Ponnalagu M et al. Ocular stem cells: a status update. Stem Cell Res Ther 2014;5:56.

8 Jeganathan VS, Palanisamy M. Treatment viability of stem cells in ophthalmology. Curr Opin Ophthalmol 2010;21:213–217.

9 Ramachandran C, Basu S, Sangwan VS et al. Concise review: the coming of age of stem cell treatment for corneal surface damage. Stem Cells Transl Med 2014;3:1160–1168.

10 Funderburgh JL, Funderburgh ML, Du Y. Stem cells in the limbal stroma. Ocul Surf 2016;14:113–120.

11 Pinnamaneni N, Funderburgh JL. Concise review: Stem cells in the corneal stroma. Stem Cells 2012;30:1059–1063.

12 Le Blanc K. Immunomodulatory effects of fetal and adult mesenchymal stem cells. Cytotherapy 2003;5:485–489.

13 Le Blanc K, Mougiakakos D. Multipotent mesenchymal stromal cells and the innate immune system. Nat Rev Immunol 2012;12:383–396.

14 Eom YW, Shim KY, Baik SK. Mesenchymal stem cell therapy for liver fibrosis. Korean J Intern Med 2015;30:580–589.

15 Lee RH, Pulin AA, Seo MJ et al. Intravenous hMSCs improve myocardial infarction in mice because cells embolized in lung are activated to secrete the anti-inflammatory protein TSG-6. Cell Stem Cell 2009;5:54–63.

16 Ortiz LA, Gambelli F, McBride C et al. Mesenchymal stem cell engraftment in lung is enhanced in response to bleomycin exposure and ameliorates its fibrotic effects. Proc Natl Acad Sci U S A 2003;100:8407–8411.

17 Reinders ME, de Fijter JW, Rabelink TJ. Mesenchymal stromal cells to prevent fibrosis in kidney transplantation. Curr Opin Organ Transplant 2014;19:54–59.

18 Shafiq M, Lee SH, Jung Y et al. Strategies for recruitment of stem cells to treat myocardial infarction. Curr Pharm Des 2015; 21:1584–1597.

19 Isern J, Mendez-Ferrer S. Stem cell interactions in a bone marrow niche. Curr Osteoporos Rep 2011;9:210–218.

20 Tsuji H, Miyoshi S, Ikegami Y et al. Xenografted human amniotic membrane-derived mesenchymal stem cells are immunologically tolerated and transdifferentiated into cardiomyocytes. Circ Res 2010;106:1613–1623.

21 Chang CJ, Yen ML, Chen YC et al. Placenta-derived multipotent cells exhibit immunosuppressive properties that are enhanced in the presence of interferon-gamma. Stem Cells 2006;24:2466–2477.

22 Parolini O, Alviano F, Bagnara GP et al. Concise review: isolation and characterization of cells from human term placenta: outcome of the first international Workshop on Placenta Derived Stem Cells. Stem Cells 2008;26: 300–311.

23 Zeng W, Li Y, Zeng G et al. Transplantation with cultured stem cells derived from the human amniotic membrane for corneal alkali burns: an experimental study. Ann Clin Lab Sci 2014;44:73–81.

24 Phinney DG, Prockop DJ. Concise review: mesenchymal stem/multipotent stromal cells: the state of transdifferentiation and modes of tissue repair--current views. Stem Cells 2007;25:2896–2902.

25 Griffith GL, Wirostko B, Lee HK et al. Treatment of corneal chemical alkali burns with a crosslinked thiolated hyaluronic acid film. Burns 2018;44:1179–1186.

26 Chavez-Garcia C, Jimenez-Corona A, Graue-Hernandez EO et al. Ophthalmic indications of amniotic membrane transplantation in Mexico: an eight years Amniotic Membrane Bank experience. Cell Tissue Bank 2016;17:261–268.

27 Barbati A, Grazia Mameli M, Sidoni A et al. Amniotic membrane: separation of amniotic mesoderm from amniotic epithelium and isolation of their respective mesenchymal stromal and epithelial cells. Curr Protoc Stem Cell Biol 2012; Chapter 1: Unit 1E 8

28 Alviano F, Fossati V, Marchionni C et al. Term Amniotic membrane is a high throughput source for multipotent Mesenchymal Stem Cells with the ability to differentiate into endothelial cells in vitro. BMC Dev Biol 2007;7:11.

29 Magana-Guerrero FS, Dominguez-Lopez A, Martinez-Aboytes P et al. Human amniotic membrane mesenchymal stem cells inhibit neutrophil extracellular traps through TSG-6. Sci Rep 2017;7:12426.

30 Deutsch TA, Hughes WF. Suppressive effects of indomethacin on thermally induced neovascularization of rabbit corneas. Am J Ophthalmol 1979;87:536–540.

31 Fantes FE, Hanna KD, Waring GO 3rd et al. Wound healing after excimer laser keratomileusis (photorefractive keratectomy) in monkeys. Arch Ophthalmol 1990;108: 665–675.

32 Ma D, Chen CB, Liang J et al. Repeatability, reproducibility and agreement of intraocular pressure measurement in rabbits by the TonoVet and Tono-Pen. Sci Rep 2016; 6:35187.

33 Nauseef WM. Isolation of human neutrophils from venous blood. Methods Mol Biol 2014;1124:13–18.

34 Neumann A, Berends ET, Nerlich A et al. The antimicrobial peptide LL-37 facilitates the formation of neutrophil extracellular traps. Biochem J 2014;464:3–11.

35 Dominguez-Lopez A, Bautista-de Lucio VM, Serafin-Lopez J et al. Amniotic membrane modulates innate immune response inhibiting PRRs expression and NF-kappaB nuclear translocation on limbal myofibroblasts. Exp Eye Res 2014;127:215–223.

36 Arnalich-Montiel F, Pastor S, Blazquez-Martinez A et al. Adipose-derived stem cells are a source for cell therapy of the corneal stroma. Stem Cells 2008;26:570–579.

37 Coulson-Thomas VJ, Caterson B, Kao WW. Transplantation of human umbilical mesenchymal stem cells cures the corneal defects of mucopolysaccharidosis VII mice. Stem Cells 2013;31:2116–2126.

38 Gomes JA, Geraldes Monteiro B, Melo GB et al. Corneal reconstruction with tissue-engineered cell sheets composed of human immature dental pulp stem cells. Invest Ophthalmol Vis Sci 2010;51:1408–1414.

39 Joyce NC, Harris DL, Markov V et al. Potential of human umbilical cord blood mesenchymal stem cells to heal damaged corneal endothelium. Mol Vis 2012;18:547–564.

40 Ma Y, Xu Y, Xiao Z et al. Reconstruction of chemically burned rat corneal surface by bone marrow-derived human mesenchymal stem cells. Stem Cells 2006;24:315–321.

41 Zhang D, Jiang M, Miao D. Transplanted human amniotic membrane-derived mesenchymal stem cells ameliorate carbon tetrachloride-induced liver cirrhosis in mouse. PLoS One 2011;6:e16789.

42 Muinos-Lopez E, Hermida-Gomez T, Fuentes-Boquete I et al. Human amniotic mesenchymal stromal cells as favorable source for cartilage repair. Tissue Eng Part A 2017;23:901–912.

43 Ren G, Chen X, Dong F et al. Concise review: mesenchymal stem cells and translational medicine: emerging issues. Stem Cells Transl Med 2012;1:51–58.

44 Ahmed SK, Soliman AA, Omar SM et al. Bone marrow mesenchymal stem cell transplantation in a rabbit corneal alkali burn model (a histological and immune histo-chemical study). Int J Stem Cells 2015;8: 69–78.

45 Holan V, Trosan P, Cejka C et al. A comparative study of the therapeutic potential of mesenchymal stem cells and limbal epithelial stem cells for ocular surface reconstruction. Stem Cells Transl Med 2015;4:1052–1063.

46 Wirbelauer C, Winkler J, Bastian GO et al. Histopathological correlation of corneal diseases with optical coherence tomography. Graefes Arch Clin Exp Ophthalmol 2002;240: 727–734.

47 Roubeix C, Godefroy D, Mias C et al. Intraocular pressure reduction and neuroprotection conferred by bone marrow-derived mesenchymal stem cells in an animal model of glaucoma. Stem Cell Res Ther 2015;6:177.

48 Stefan C, Timaru CM, Iliescu DA et al. Glaucoma after chemical burns and radiation. Rom J Ophthalmol 2016;60:209–215.

49 Manuguerra-Gagne R, Boulos PR, Ammar A et al. Transplantation of mesenchymal stem cells promotes tissue regeneration in a glaucoma model through laser-induced paracrine factor secretion and progenitor cell recruitment. Stem Cells 2013;31:1136–1148.

50 Jester JV, Barry PA, Lind GJ et al. Corneal keratocytes: in situ and in vitro organization of cytoskeletal contractile proteins. Invest Ophthalmol Vis Sci 1994;35:730–743.

51 Torricelli AA, Santhanam A, Wu J et al. The corneal fibrosis response to epithelial-stromal injury. Exp Eye Res 2016; 142:110–118.

52 Singh V, Torricelli AA, Nayeb-Hashemi N et al. Mouse strain variation in SMA(+) myofibroblast development after corneal injury. Exp Eye Res 2013;115:27–30.

53 Li W, He H, Chen YT et al. Reversal of myofibroblasts by amniotic membrane stromal extract. J Cell Physiol 2008;215:657–664.

54 Brinkmann V, Reichard U, Goosmann C et al. Neutrophil extracellular traps kill bacteria. Science 2004;303:1532–1535.

55 Fuchs TA, Abed U, Goosmann C et al. Novel cell death program leads to neutrophil

extracellular traps. J Cell Biol 2007;176: 231–241.

56 Sonawane S, Khanolkar V, Namavari A et al. Ocular surface extracellular DNA and nuclease activity imbalance: a new paradigm for inflammation in dry eye disease. Invest Ophthalmol Vis Sci 2012;53:8253–8263.

57 Barliya T, Dardik R, Nisgav Y et al. Possible involvement of NETosis in inflammatory processes in the eye: Evidence from a small cohort of patients. Mol Vis 2017;23:922–932.

58 Jarrot PA, Kaplanski G. Pathogenesis of ANCA-associated vasculitis: An update. Autoimmun Rev 2016;15:704–713.

59 Bian F, Pelegrino FS, Pflugfelder SC et al. Desiccating Stress-Induced MMP Production and Activity Worsens Wound Healing in Alkali-Burned Corneas. Invest Ophthalmol Vis Sci 2015;56:4908–4918.

60 Bian F, Pelegrino FS, Henriksson JT et al. Differential Effects of Dexamethasone and Doxycycline on Inflammation and MMP Production in Murine Alkali-Burned Corneas Associated with Dry Eye. Ocul Surf 2016;14: 242–254.

61 Kim JA, Ko JH, Ko AY et al. TSG-6 protects corneal endothelium from transcorneal cryoinjury in rabbits. Invest Ophthalmol Vis Sci 2014;55:4905–4912.

See www.StemCellsTM.com for supporting information available online.